DOI: 10.1002/chem.200600328

Quasilinear Molecule par Excellence, $SrCl_2$: Structure from High-Temperature Gas-Phase Electron Diffraction and Quantum-Chemical Calculations—Computed Structures of $SrCl_2$·Argon Complexes

Zoltán Varga,[a] Giuseppe Lanza,[b] Camilla Minichino,[b] and Magdolna Hargittai*[a]

Abstract: The molecular geometry of strontium dichloride has been determined by high-temperature electron diffraction (ED) and computational techniques. The computation at the MP2 level of theory yields a shallow bending potential with a barrier of about 0.1 kcal mol^{-1} at the linear configuration. The experimentally determined thermal average Sr−Cl bond length, r_g, is 2.625 ± 0.010 Å and the bond angle, $\measuredangle_a$, is 142.4 ± 4.0°. There is excellent agreement between the equilibrium bond lengths estimated from the experimental data, 2.607 ± 0.013 Å, and computed at different levels of theory and basis sets, 2.605 ± 0.006 Å. Based on anharmonic analyses of the symmetric and asymmetric stretching as well as the bending motions of the molecule, we estimated the thermal average structure from the computation for the temperature of the ED experiment. In order to emulate the effect of the matrix environment on the measured vibrational frequencies, a series of complexes with argon atoms, $SrCl_2{\cdot}Ar_n$ (n = 1–7), with different geometrical arrangements were calculated. The complexes with six or seven argon atoms approximate the interaction best and the computed frequencies of these molecules are closer to the experimental ones than those computed for the free $SrCl_2$ molecule.

Keywords: ab initio calculations · alkaline-earth dihalides · quasilinear molecules · strontium · structure elucidation

Introduction

Alkaline-earth dihalides, despite their simple stoichiometry, are unusual systems. Simple models, such as the VSEPR model[1] or Walsh diagrams,[2] otherwise successfully predicting and explaining molecular shapes, fail here. All alkaline-earth dihalides should be linear according to these models, but as different experimental and computational results suggest, some of them do not conform with this expected behavior. An increasing amount of evidence has suggested that in addition to the clearly linear molecules[3–6] some alkaline-earth dihalides are bent[7] and others might best be described as quasilinear[8] (for a review of these structures see, e.g., refs. [9–12]). There is no strict definition of quasilinearity, but for a working definition, a molecule is quasilinear if it has a very flat bending potential and a barrier at the linear configuration lower than or about as large as the value of its bending frequency. Quasilinear molecules are difficult objects to investigate both theoretically and experimentally for a variety of reasons: in the experimental investigations, it is the low volatility and consequently the need for high-temperature experiments on the one hand and their very large amplitude vibrations on the other that cause the difficulties; in computations, beside the obvious problems due to the size of some of the atoms, the major difficulty is the very flat nature of the bending potential. Both techniques encounter difficulties as a result of the anharmonic nature of the vibrations of these molecules.

The most problematic molecules as far as their shapes are concerned are calcium difluoride and the strontium dihalides. CaF_2 has been the object of many computational stud-

---

[a] Z. Varga, Prof. Dr. M. Hargittai
Structural Chemistry Research Group of the Hungarian Academy of Sciences
Eötvös University, Pf. 32, 1518 Budapest (Hungary)
Fax: (+36) 1-372-2730
E-mail: hargitta@chem.elte.hu

[b] Prof. G. Lanza, Prof. C. Minichino
Dipartimento di Chimica, Universita' della Basilicata
Via N. Sauro 85, 85100 Potenza (Italy)

Supporting information for this article is available on the WWW under http://www.chemeurj.org/ or from the author. Electron diffraction molecular intensities for two camera ranges, computed Mulliken charges for $SrCl_2$ and its complexes with argon, $SrCl_2{\cdot}Ar_n$ (n = 1–7), Cartesian coordinates for the $SrCl_2{\cdot}Ar_n$ complexes (n = 1–6; for the group **C** structures also for n = 7), vibrational frequencies for the complexes for n = 1–4 and for group **B** $SrCl_2{\cdot}Ar_6$, and the estimation procedure for the suggested computed equilibrium bond length and bond angle of $SrCl_2$ with their standard deviation.

ies, the latest of which is the study by Koput and Roszczak;[13] for references to the earlier ones see ref. [9]. $SrBr_2$ has already been subjected to detailed experimental[8] and computational[10,11] studies. The available information about the geometry of $SrCl_2$ is ambiguous. A short conference abstract of an earlier electron diffraction investigation[14] suggested a bent equilibrium structure with a bond angle of 142 ± 8°, but a full report never appeared. The results of previous quantum chemical calculations[10,11] were not conclusive as they very much depended on the level of the calculation. There have been three infrared spectroscopic studies of $SrCl_2$; one of them in the gas phase[15] and the other two in matrices, one an argon matrix[16] and the other a krypton matrix.[17] The gas-phase study indicated a linear structure, while the two others suggested a bent geometry with a bond angle of 130 ± 5° and 118 ± 5°, respectively.

Abstract in Hungarian: *Meghatároztuk a stroncium-diklorid molekula szerkezetét magashõmérsékletû elektrondiffrakcióval (ED) és kvantumkémiai számításokkal. MP2 számítások alapján a hajlítási potenciálnak kb. 0.1 kcal mol*$^{-1}$ *magasságú gátja van a lineáris konfigurációnál. A kísérletileg meghatározott hõmérsékletre átlagolt Sr–Cl kötéshossz,* r_g*, 2.625 ± 0.010 Å és a kötésszög 142.4 ± 4.0°. A kísérlet alapján becsült egyensúlyi kötéstávolság, 2.607 ± 0.013 Å, kiválóan egyezik a különbözõ szint'û számításokkal kapott értékkel, 2.605 ± 0.006 Å. Elvégeztük a molekula szimmetrikus és aszimmetrikus nyújtásának valamint hajlítási mozgásának anharmonikus analízisét és ennek alapján megbecsültük a kísérlet hõmérsékletére átlagolt molekulaszerkezetet is. A stroncium-diklorid különbözǫõ számú argon atommal képzett komplexeinek,* $SrCl_2{\cdot}Ar_n$ *(n=1–7), a szerkezetét is kiszámítottuk, azzal a céllal, hogy a mátrix környezet hatását a mátrix-izolációs rezgési spektroszkópiával mért frekvenciákra megbecsülhessük. A 6 és 7 argon atomot tartalmazó komlexek közelítik legjobban a valóságos állapotot és az ezekre számított frekvenciák jobban egyeznek a kísérletiekkel, mint a szabad* $SrCl_2$ *molekulára számítottak.*

Abstract in Italian: *La geometria molecolare del cloruro di stronzio è stata determinata tramite diffrazione elettronica ad alta temperatura e tecniche computazionali. La curva di potenziale valutata a livello MP2 per il moto di piegamento è molto piatta e la barriera rispetto alla configurazione lineare è di circa 0.1 kcal mol*$^{-1}$*. I valori termici medi determinati sperimentalmente per la lunghezza di legame Sr–Cl,* r_g*, e per l'angolo di legame,* $\angle_a$*, sono, rispettivamente, 2.625 ± 10 Å e 142.4 ± 4.0°. Da calcoli effettuati a vari livelli di teoria ed impiegando differenti basi si ottiene una lunghezza di legame di equilibrio di 2.605 ± 0.006 Å. Tale lunghezza di legame è in eccellente accordo con quella determinata sperimentalmente (2.607 ± 0.013 Å). La struttura termica media della molecola, valutata alla temperatura degli esperimenti di diffrazione elettronica, è stata stimata includendo esplicitamente l'anarmonicità dei moti di piegamento, di stiramento simmetrico e asimmetrico. Allo scopo di simulare l'effetto della matrice sulle frequenze vibrazionali, sono stati presi in esame una serie di complessi di* $SrCl_2$ *con atomi di argon,* $SrCl_2{\cdot}Ar_n$ *(n=1–7), in differenti disposizioni geometriche. I complessi con 6 e 7 atomi di argon simulano meglio l'interazione matrice-molecola e le frequenze calcolate per* $SrCl_2$ *"incapsulata" sono piû vicini ai dati sperimentali rispetto a quelle calcolate per la molecola libera.*

As $SrCl_2$ is a crucial molecule among the alkaline-earth dihalides, we decided to determine its structure by high-temperature electron diffraction and high-level computational techniques. The physical meaning of the geometries determined by electron diffraction and computations are different[18] and this difference is especially important for such a floppy molecule as $SrCl_2$. Therefore, we tried to make the two techniques compatible with each other in two ways; from the computational point of view, we calculated the thermal average structure of the molecule for both the low-frequency bending and the symmetric stretching modes; and from the electron diffraction point of view, we estimated the experimental equilibrium geometry by applying anharmonic vibrational corrections to the thermal average structure.

Most of the available vibrational spectroscopic information about $SrCl_2$ comes from matrix isolation experiments.[16,17] The gas-phase molecule is very reactive owing to its strong Lewis acid character. This suggests that $SrCl_2$ molecules might interact with matrix atoms causing structural changes within the molecule. In order to look into this question, we performed a series of calculations in which we simulated the matrix environment by placing argon atoms around the $SrCl_2$ molecule, $SrCl_2{\cdot}Ar_n$ (n = 1–7), and calculated the structures and vibrational frequencies of these species.

Computational Details

Computational studies of the $SrCl_2$ molecule are not as straightforward as one would expect based on its simple stoichiometry. It is very clear that the computed bond length of a molecule depends on the method and basis sets applied, but it is not so clear that this applies to the shape of the molecule as well. Kaupp et al.[10] found that the $SrCl_2$ molecule adopts a linear shape at the RHF level of theory when a contraction[3d,2d] of the "d" space is used, but the molecule becomes bent (167.3°) when the d shell is uncontracted. Further bending was observed when electronic correlation effects were included. Our preliminary calculations with different methods also showed that the d space has to be uncontracted in order to obtain reliable results for these types of molecules. Furthermore, it is also essential to take electron correlation into account.

Our computations were carried out at the MP2 (full) level of theory, with all electrons correlated. The reliability of the MP2 method is well established, and its good computational performance allowed us to treat systems with as many as 729 basis functions (in the $SrCl_2{\cdot}Ar_n$ complexes). At the same time, we did not want to rely on only one method, therefore, a few calculations were also carried out by using a density functional method (B3PW91) and also by using the CCSD and CCSD(T) methods. Geometries and harmonic vibrational frequencies were obtained by using standard numerical gradient techniques. Basis set superposition error (BSSE) was estimated by the counterpoise method for calculating the stabilization energies of the $SrCl_2{\cdot}Ar_n$ complexes. All electronic structure calculations were performed by using the Gaussian 03 program package.[19]

After initial trial calculations with the shape-consistent effective core potentials (ECP) developed by Hay and Wadt,[20] we chose the energy-adjusted quasirelativistic ECP developed by the Stuttgart group (ST)[21] to describe the strontium atom core; it incorporates scalar relativistic effects. This ECP explicitly treats semicore 4s and 4p electrons ([Ar]$3d^{10}$). We started with the basis set originally published with the ST ECP, but uncontracted the d functions so we had the following construction scheme for the s, p, and d functions: [3111,3111,11111]. Chlorine is a light enough atom to be treated at the nonrelativistic level and it was described by all-electron basis sets. Huzinaga's all-electron (12s, 9p) basis sets contracted as [631111,52111] by McLean and Chandler[22] were chosen as the starting point.

As our previous experience has shown, rather large basis sets are needed for both the metal and the halogen atoms to obtain converged bond lengths for the metal halides.[5a,23] Therefore, we tried to improve the basis sets by adding new polarization functions to them. The Gaussian exponents of these polarization functions were optimized by MP2 single-point energy calculations. As a first step, two f polarization functions were added to strontium ($\alpha_{1f}=1.0$, $\alpha_{2f}=0.5$) and one sp diffuse function and two d and one f polarization functions to chlorine ($\alpha_{sp}=0.0483$, $\alpha_{1d}=1.05$, $\alpha_{2d}=0.35$, $\alpha_{1f}=0.7$). Next we improved the basis sets step by step up to 4f3g on strontium ($\alpha_{3f}=0.18$, $\alpha_{4f}=0.085$, $\alpha_{1g}=1.1$, $\alpha_{2g}=0.3$, $\alpha_{3g}=0.12$) and up to 3d2f1g on chlorine ($\alpha_{3d}=12.5$, $\alpha_{2f}=0.2$, $\alpha_{1g}=1.6$). We also checked the effect of using another basis set for the chlorine atom, namely the standard cc-pVXZ sets of Woon and Dunning up to the quintuple-zeta level.[24] For the latter calculations we extended the strontium basis to 4f3g2h ($\alpha_{3g}=1.8$, $\alpha_{1h}=1.23$, $\alpha_{2h}=2.0$), for which the α_{3g} exponent was reoptimized after adding the α_{1h} exponent. The highest-level basis set was of 4f3g2h1i quality on strontium ($\alpha_{1i}=1.3$) with the cc-pV-(6+d)Z[25] basis set on chlorine. For the $SrCl_2{\cdot}Ar_n$ complexes the all-electron McLean–Chandler basis functions were used[22] augmented by two d, two f, one g and one diffuse sp functions for argon and chlorine (Ar: $\alpha_{d1}=1.20$, $\alpha_{d2}=0.425$, $\alpha_{f1}=1.0$, $\alpha_{f2}=0.5$, $\alpha_{g}=1.1$, $\alpha_{sp}=0.06$; Cl: $\alpha_{d1}=1.05$, $\alpha_{d2}=0.35$, $\alpha_{f1}=0.7$, $\alpha_{f2}=0.2$, $\alpha_{g}=0.8$, $\alpha_{sp}=0.0483$). For strontium, the [3111,3111,11111] basis set was complemented with two f and one g polarization functions ($\alpha_{f1}=1.0$, $\alpha_{f2}=0.5$, $\alpha_{g}=1.1$).

Six d-type, 10 f-type, 15 g-type, 21 h-type, and 28 i-type Cartesian Gaussian basis functions were used. These give additional flexibility to the basis set because a single exponent α_d function is associated with five d-type and one s-type pure spherical Gaussian functions, a single exponent α_f is associated with seven f-type and three p-type functions, and a single exponent α_g is associated with nine g-type, five d-type, and one s-type functions. For the h functions, a single exponent α_h is associated with eleven h, seven f, and three p functions and for the i function a single exponent α_i is associated with 13 i functions, nine g-, five d-, and one s-type functions.

To bring our experimental electron diffraction and computational results on the structure of $SrCl_2$ to a common denominator, we calculated the thermal average structure of the molecule at the temperature of the electron diffraction experiment. For this, we had to describe the anharmonicity of the vibrations (both stretching and bending) and also to approximate the large amplitude motion of the molecule. The large amplitude motion along the double-minimum potential well of the bending mode was described by an effective one-dimensional Hamiltonian. The nuclear motions were analyzed in the framework of the so-called distinguished coordinate approach.[26] The bending path was obtained through optimization of the bond length, r(Sr–Cl), for selected values of the bond angle, $\measuredangle$Cl–Sr–Cl, as the representative of the large amplitude motion. The symmetric and asymmetric stretching motions were also analyzed in the framework of a one-dimensional Hamiltonian. In these cases, the r(Sr–Cl) bond length was chosen as the representative coordinate.

The one-dimensional variational problem can be solved by numerical integration for any vibrational number n and we obtain n eigenstates with their eigenvalues ε_n. By assuming a Boltzmann distribution of the eigenstates and anharmonic vibrational frequencies derived from the one-dimensional Hamiltonian the thermal average angle, $\langle\Theta\rangle_T$, and the thermal average bond length along the bending motion, $\langle r_b\rangle_T$, and the thermal average bond length along the symmetric, $\langle r_s\rangle_T$, and asymmetric, $\langle r_a\rangle_T$, stretching were computed as a function of temperature. The variational solution of the effective one-dimensional problem is obtained by using evenly spaced cubic b-splines both as basis functions and to interpolate the potential energy curves. To obtain reliable high-energy eigenstates that are significantly populated in the experimental ED measurement (up to 10 kcal mol^{-1}), it is important to include potential points that cover higher energy regions (up to 20 kcal mol^{-1}).

Experimental Section

Solid samples were evaporated from a molybdenum nozzle at a temperature of 1500 ± 50 K in our combined electron diffraction-quadrupole mass spectrometric experiment developed in the Budapest laboratory[27] using the modified EG-100A apparatus.[28] The accelerating voltage was 60 kV. The mass spectra gave no indication of having other than monomeric $SrCl_2$ molecules in the vapor. Special thin sheets of molybdenum were used to shield the high-temperature nozzle so that the light emitted by it should not influence the emulsion of the photoplate. Even with these precautions, this could not be completely avoided for the short camera range (19 cm) experiments and the signal-to-noise ratio of the outer range of these plates was worse than usual. The electron-scattering functions from reference [29] were used. Electron diffraction patterns were taken at 50 (four plates) and 19 cm (four plates) camera distances. The data intervals were 2.00–14.00 Å^{-1} (with 0.125 Å^{-1} steps) and 9.00–26.00 Å^{-1} (with 0.25 Å^{-1} steps) for the two camera ranges, respectively. These have been deposited as Supporting Information. Figure 1 presents the experimental and theoretical molecular intensity curves, and Figure 2 the corresponding radial distributions.

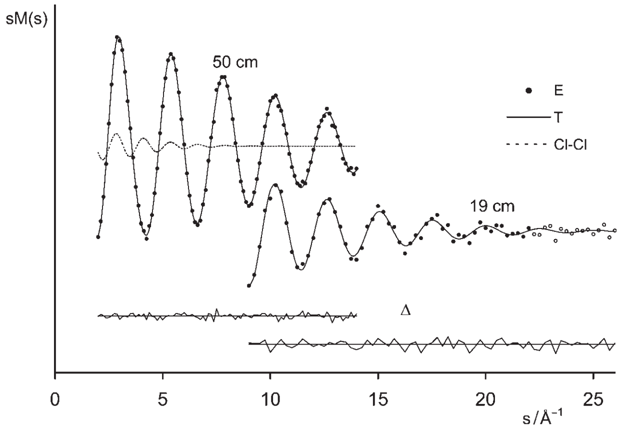

Figure 1. Experimental and theoretical molecular intensities and their difference curves for $SrCl_2$. The contribution of the Cl···Cl distance to the total intensity is also indicated. The open circles indicate those experimental data that were taken into consideration with a smaller weight.

Structure Analysis and Results

Computations of $SrCl_2$: The computed geometrical parameters and vibrational frequencies of the $SrCl_2$ molecule are collected in Table 1. All calculations resulted in bent geometries except those MP2 and CCSD(T) calculations in which the chlorine atoms were described by the cc-pVQZ quadruple-zeta basis set of Woon and Dunning.[24] This happened

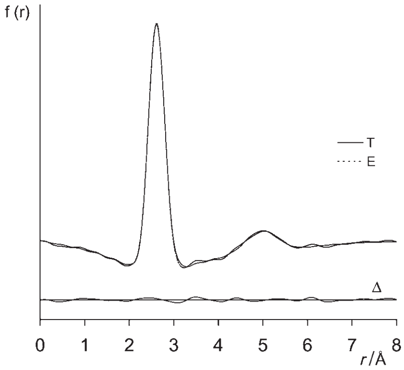

Figure 2. Experimental and theoretical radial distributions and their differences for $SrCl_2$.

in combination with different basis sets on strontium (for MP2). Therefore, it must be the result of the chlorine basis set, or its combination with the MP2 and CCSD(T) methods (see Table 1). Interestingly, the other Woon and Dunning basis sets on chlorine, either the triple-zeta or the quintuple-zeta, gave bent geometries that were consistent with the results of other calculations. All density functional calculations, including the ones with the cc-pVQZ basis set on chlorine, resulted in bent geometries. The Cl-Sr-Cl bond angle in the bent structures varied between 149 and 156°, which, considering the fluxionality of the $SrCl_2$ molecule along the bending motion, is a surprisingly small interval. Even more interesting is that there does not seem to be any apparent trend in the variation of the bond angle with increasing basis set. The same is true for the variation of the bond length which changed within 0.01 Å.

The geometries computed by one particular method with different basis sets scatter even less. The bond angles vary within 5° for the MP2 method, while the bond-length change is the same as above. The density functional results are even more consistent; the bond angles vary within 3°, from 149 to 152°, and the bond lengths within 0.005 Å. The density functional method gives smaller bond angles and larger bond lengths than the MP2 method. We carried out only a couple of CCSD and CCSD(T) calculations with relatively small basis sets and therefore the performance of these methods cannot be discussed fairly.

Table 1. Computed geometrical parameters and harmonic vibrational frequencies (with IR intensities [km mol^{-1}] in parentheses) of the $SrCl_2$ molecule. Experimental data are given for comparison.

Method	Basis set (Sr/Cl)[a]	Sr–Cl [Å]	∡Cl-Sr-Cl [°]	ν_1 [cm^{-1}]	ν_2 [cm^{-1}]	ν_3 [cm^{-1}]
B3PW91	2f/MC-2d1f	2.603	149.1			
B3PW91	2f/cc-pVTZ	2.603	148.9			
B3PW91	3f2g/MC-3d2f1g	2.606	150.3	273.1(8)	24.1(35)	316.0(162)
B3PW91	3f2g/cc-pVQZ	2.606	148.9			
B3PW91	4f3g1h/cc-pV5Z	2.606	148.9	272.9(8)	25.6(34)	315.5(156)
MP2	2f/MC-2d1f	2.605	152.4			
MP2	2f/cc-pVTZ	2.604	152.8			
MP2	3f2g/MC-3d2f1g	2.598	154.0	278.5(7)	27.3(39)	328.2(160)
MP2	3f2g/cc-pVQZ	2.602	180.0			
MP2	4f3g/cc-pVQZ	2.600	180.0			
MP2	4f3g1h/cc-pVQZ	2.598	180.0			
MP2	4f3g1h/cc-pV5Z	2.601	155.6	275.5(6)	25.5(39)	325.4(157)
MP2	4f3g2h/cc-pV5Z	2.599	154.1			
MP2	4f3g2h1i/cc-pV(6+d)Z	2.595	155.0			
CCSD	2f/MC-2d1f	2.618	155.5			
CCSD	2f/cc-pVTZ	2.618	156.3			
CCSD(T)	2f/MC-2d1f	2.613	153.2			
CCSD(T)	2f/cc-pVTZ	2.613	154.0			
CCSD(T)	3f2g/MC-3d2f1g	2.607	155.6			
CCSD(T)	3f2g/cc-pVQZ	2.610	180.0			
	suggested equilibrium parameters[b]	2.605 ± 0.006	153.5 ± 2.6			
	exp. ED[c]	2.607 ± 0.013				
	exp. ED[d]	2.606 ± 0.008				
MP2	4f3g1h/cc-pV5Z[e]	2.613				
B3PW91	4f3g1h/cc-pV5Z[e]	2.618				
MP2	4f3g1h/cc-pV5Z[f]	2.593	146.5			
B3PW91	4f3g1h/cc-pV5Z[f]	2.601	144.9			
	exp. ED	2.625 ± 0.010	142.4 ± 4.0			
	exp. IR (gas)[g]					300(7)
	exp. IR (Ar)[h]		130 ± 5	275		308.0
	exp. IR (Kr)[i]		118 ± 5	269.3		299.5
	estimated gas-phase[h]			285 ± 10		318 ± 10
	estimated gas-phase[j]			287		324

[a] For definition of the basis sets see the Computational Section. [b] Only bent structures are considered. For the estimation procedure, see the text and Supporting Information. [c] Experimental equilibrium bond length estimated by Morse-type anharmonic corrections. [d] Experimental equilibrium bond length from joint ED-SP analysis (see text for details). [e] Computed thermal average structure for the symmetric stretching at 1500 K. [f] Computed thermal average structure for the bending at 1500 K. [g] Ref. [15]. [h] Ref. [16]. [i] Ref. [17]. [j] Ref. [9].

The computed harmonic symmetric stretching frequencies depend only slightly on the method and basis set applied and are about 10 cm^{-1} lower than the estimated experimental gas-phase frequencies. At the same time, the asymmetric stretching frequency computed by the B3PW91 method is about 10 cm^{-1} smaller than that determined by the MP2 method and this seems to be independent of the basis sets applied. The density functional asymmetric stretching frequency is closer to the experimental one than the MP2 value.

The potential energy curves along the ν_1 and ν_3 stretches appear parabolic and the harmonic frequencies could be accepted as reasonable estimates of the vibrational transitions. The MP2/4f3g1h/cc-pV5Z potential energy curve for the symmetric stretching is shown in Figure 3a. The curve could be fitted up to about 5 kcal mol^{-1} in terms of changes in the bond distance, Δr, by a third-degree polynomial [Eq. (1)].

$$E = 218.9\Delta r^2 - 239.4\Delta r^3 \qquad (1)$$

The polynomial for the B3PW91/4f3g1h/cc-pV5Z potential energy curve is given by Equation (2)(the transitions are given in parentheses in Figure 3a).

$$E = 209.6\Delta r^2 - 236.3\Delta r^3 \qquad (2)$$

The curve exhibits the classical asymmetric form with respect to the equilibrium position (see Figure 3a) and the vibrational levels crowd more closely together with increasing vibrational number n. Note that the 0→1 fundamental transition is smaller than the harmonic frequency [271.8 (MP2) vs. 275.5 cm^{-1}], thus indicating a noticeable anharmonicity even at the bottom of the well. The probability distributions of each vibrational level are slightly skewed in such a way that they have greater magnitude on the side of the well corresponding to bond stretching. This skewing towards increasing r(Sr–Cl) implies that the average internuclear position increases with increasing quantum numbers. Thus, at a high temperature, when vibrational states with high quantum numbers are significantly populated (up to $n = 9$), corresponding to the ED experimental conditions, the thermal average bond length along the symmetric stretching mode will be longer than the equilibrium bond length (by 0.012 Å, by both methods, see Table 1).

The asymmetric stretching potential energy curve (see Figure 3b) could be fitted adequately (up to 5 kcal mol^{-1}) in terms of changes in the bond distance by even fourth-degree polynomials [Eq. (3) and Eq. (4)].

$$\text{MP2}: \; E = 177.1\Delta r^2 + 184.9\Delta r^4 \qquad (3)$$

$$\text{B3PW91}: \; E = 161.4\Delta r^2 + 437.7\Delta r^4 \qquad (4)$$

Chemical intuition would suggest a flatter potential energy curve with increasing distance from the center, and consequently, a decrease of the vibrational steps. In contrast to this, we found a positive sign for the quartic term suggesting a small increase in the vibrational step with increasing quantum number. However, the corrections of the harmonic frequencies are small and the probability distribution of each vibrational level is perfectly symmetric. These data indicate that if the asymmetric stretching contributes to the thermal average bond length, it only happens at the second

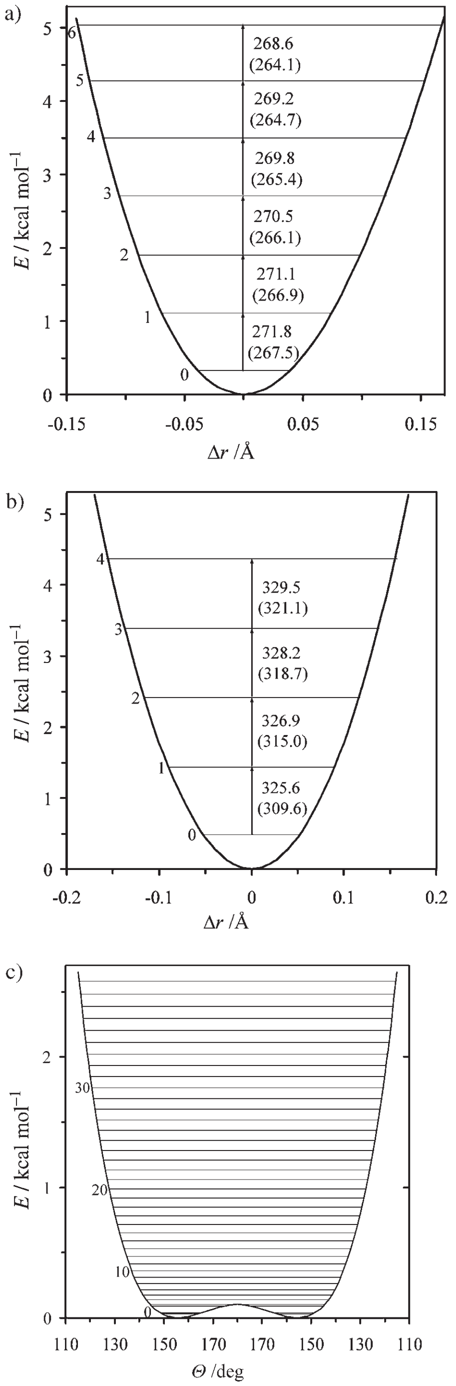

Figure 3. a) The potential energy curve for symmetric stretching in $SrCl_2$. b) The potential energy curve for asymmetric stretching. c) The potential energy curve along the ν_2 bending mode. All at the MP2//4f3g1h/cc-pV5Z level, with the B3PW91 results given in parentheses for (a) and (b).

level, that is, throughout its coupling with other normal modes.

The potential energy curve along the ν_2 bending mode is strongly anharmonic (Figure 3c) and in the low potential energy region ($<5\,\mathrm{kcal\,mol^{-1}}$) it could be fitted adequately in terms of changes in the bond angle, $\Delta\Theta$, only by even tenth-degree polynomials [Eq. (5) and Eq. (6)].

$$\begin{aligned}\text{MP2}:\ E &= 0.10-3.42\times10^{-4}\Delta\Theta^2+3.06\times10^{-7}\Delta\Theta^4\\ &-2.99\times10^{-11}\Delta\Theta^6+3.02\times10^{-15}\Delta\Theta^8-1.19\times10^{-19}\Delta\Theta^{10}\end{aligned}\tag{5}$$

$$\begin{aligned}\text{B3PW91}:\ E &= 0.28-5.79\times10^{-5}\Delta\Theta^2+2.86\times10^{-7}\Delta\Theta^4\\ &-1.50\times10^{-11}\Delta\Theta^6+1.71\times10^{-15}\Delta\Theta^8-1.36\times10^{-19}\Delta\Theta^{10}\end{aligned}\tag{6}$$

Anharmonic vibrational frequencies, computed using the effective one-dimensional Hamiltonian, show the phenomenon of quantum mechanical tunneling with consequent doubling of the vibrational levels. Nevertheless, not considering the low-lying levels, the vibrational step increases with increasing quantum number. For low-lying levels the maxima of the probability distribution are located in the 140–180° bond angle range, while, for excited states, the absolute maxima move towards the potential energy walls (smaller bond angles), thus causing a significant reduction of the average bond angles. By assuming a Boltzmann population of the eigenstates for the large amplitude bending motion (Figure 3c), we calculated the thermal average angle at the ED experimental temperature (1500 K) and it appears to be considerably smaller than the equilibrium bond angle. Thus the agreement between experiment and computation improves considerably [146.5 (MP2) and 144.9° (B3PW91) vs. 142.4±4.0° from the experiment]. The decrease in the bond angle along the large amplitude bending motion is accompanied by a gradual shortening of the Sr−Cl bond. This means that the thermal average distance decreases with respect to the equilibrium one and a shortening of 0.008 (MP2) or 0.005 Å (B3PW91) is computed at the experimental ED temperature.

The present one-dimensional analysis of the vibrationally averaged structure reveals that a distinct treatment is required for the three normal modes because of their different nature. On the one hand, it is reasonable to separate the "slow" large amplitude bending from the "fast" stretching modes because their effects on bending are modest and, in fact, a reasonable theoretical/experimental comparison is possible. On the other hand, the "independent vibrations" models are not appropriate for the correct description of the overall behavior of the bond distance because of the anharmonic coupling of various oscillators. In particular, two aspects seem to be critical, the shortening of the bond along the bending mode and its considerable lengthening due to the anharmonicity of the stretching. Moreover, a quantitative treatment of this problem should also take into consideration quantum mechanical tunneling.

Morse function for structure analysis: In order to have a realistic estimate of the stretching anharmonicity in the electron diffraction analysis the so-called Morse parameter for a certain bond is often approximated by assuming that it is the same as that for the corresponding diatomic molecule. We calculated the anharmonic potential of the SrCl molecule and from the computed $\omega_e=304.2\,\mathrm{cm^{-1}}$ and $D_e=103.6\,\mathrm{kcal\,mol^{-1}}$ values the Morse constant, a, was calculated to be 0.99 $\mathrm{\AA^{-1}}$. To make sure that our approximation is correct, we estimated the Morse constant for the $SrCl_2$ molecule as well. We calculated the potential energy curve for a single Sr−Cl bond stretching at the MP2/4f3g1h/cc-pV5Z level. This curve was obtained by constraining the bond angle and one of the two bond lengths at the equilibrium values while the other Sr−Cl bond length was varied. The following parameters were determined this way: $\omega_e=290.5\,\mathrm{cm^{-1}}$ and $D_e=118.2\,\mathrm{kcal\,mol^{-1}}$. The corresponding Morse parameter, a, is 0.87 $\mathrm{\AA^{-1}}$, showing that the usually applied diatomic approximation is acceptable.

Electron diffraction analysis: Strontium dichloride has low volatility; therefore very high temperatures were needed to obtain sufficient vapor pressure. The extremely high temperature of the nozzle resulted in some light in the diffraction chamber and this somewhat affected the background of the 19 cm camera-range curve. Therefore, the signal-to-noise ratio of this curve is rather poor at larger scattering angles. Thus, we used only the data up to $s=22\,\mathrm{\AA^{-1}}$ with full weight and introduced a decreasing weight for the remaining data. We also checked the effect of using an even smaller angle range in the refinement, but the parameters changed only slightly and these differences were then taken into consideration in estimating the uncertainties. The good agreement between the experimental and calculated distributions (the latter corresponding to the monomeric $SrCl_2$ molecule) supports the observation made in the quadrupole mass spectrometric experiment that there are no higher associates present in the vapor.

The thermal average bond length of the molecule could be determined with good precision. The contribution of the Cl···Cl nonbonded pair to the molecular scattering, on the other hand, is relatively small, as indicated in Figure 1. This also means that although we have a distinct peak on the radial distribution corresponding to the Cl···Cl distance (see Figure 2), it comes only from the 50-cm curve and thus carries larger uncertainty than usual. This, in turn, means that the determination of the bond angle cannot be as precise as one might wish. This problem is compounded by the fact that the electron diffraction geometries are thermal average structures and they may substantially differ from the equilibrium structures that result from the computations.

To estimate the equilibrium structure, vibrational corrections must be applied, which at this high temperature are considerable. This vibrational information may come from experimental infrared and Raman spectra or from computations. Unfortunately, the spectroscopic information in the literature is not unambiguous (vide infra). The bond angles suggested from the matrix isolation spectroscopic experiments, 130 and 118°, respectively, do not agree with our electron diffraction results, neither with the computations. One reason for this might be the relative insensitivity of the isotope-shift method for estimating bond angles; another, perhaps even more likely one, is the possible interaction of the $SrCl_2$ molecules with the matrix atoms resulting in a small distortion of the free $SrCl_2$ molecule, as will be discussed below.

The geometrical parameters determined by electron diffraction are given in Table 2. Here the estimated equilibrium bond length is also given. We estimated the equilibrium bond length in two different ways. One is with anharmonic vibrational corrections, according to the expression $r_e^M = r_g - {}^3\!/_2 a l^2$, where a is the Morse constant, the superscript M refers to the Morse potential, and l is the mean-square vibrational amplitude at the experimental temperature.[30] The other method was the so-called joint electron diffraction-vibrational spectroscopic (ED-SP) analysis.[31] In this, the electron diffraction intensities and vibrational frequencies are used together in the structure refinement based on a simple anharmonic potential. The anharmonic effects appear in both the kinetic and the potential energy parts of the vibrational Hamiltonian in this approximation. The bond lengths estimated by the two methods show remarkable agreement.

Table 2. Geometrical parameters of $SrCl_2$ from electron diffraction.[a]

Parameter	
r_g(Sr–Cl) [Å]	2.625 ± 0.010
r_e^M(Sr–Cl)[b] [Å]	2.607 ± 0.013
r_e^a(Sr–Cl)[c] [Å]	2.606 ± 0.008
l(Sr–Cl) [Å]	0.116 ± 0.003
κ(Sr–Cl) [Å^3]	(8.6±2.0) × 10^{-5}
r_g(Cl···Cl) [Å]	4.980 ± 0.039
l(Cl···Cl) [Å]	0.321 ± 0.030
$\measuredangle_a$Cl–Sr–Cl [°]	142.4 ± 4.0
$\measuredangle_e$ Cl–Sr–Cl[d] [°]	143.3 ± 3.4

[a] Error limits are estimated total errors, including systematic errors, and the effect of constraints used in the refinement: $\sigma_t = [2\sigma_{LS}^2 + (cp)^2 + \Delta^2]^{1/2}$, where σ_{LS} is the standard deviation of the least squares refinement, p is the parameter, c is 0.002 for distances and 0.02 for amplitudes, and Δ is the effect of constraints. [b] Experimental equilibrium bond length estimated by Morse-type anharmonic corrections. [c] Experimental equilibrium bond length from joint ED-SP analysis (see text for details). [d] Experimental equilibrium bond angle from joint ED-SP analysis (see text for details).

Note also that there is good agreement between the Morse constants estimated by electron diffraction (using two different methods) and those determined by computation. The Morse constant from the asymmetry parameter of the electron diffraction analysis is 0.97 ± 0.22 Å^{-1}. There is also another way to estimate the Morse constants, from the anharmonic cubic force constants based on Equation (7),

$$a = -2f_{rrr}/(f_r r_e) \tag{7}$$

where a is the Morse constant, f_{rrr} is the cubic coefficient of the anharmonic potential, f_r is the stretching force constant and r_e is the equilibrium bond length.[32] Our anharmonic joint ED-SP analysis resulted in a cubic force constant, f_{rrr}, of −1.54 ± 0.42 mdyn Å^{-1}, which corresponds to a Morse constant of 0.77 ± 0.21 Å^{-1}, again, in agreement with the two values determined from the asymmetry parameter and derived from the computation for the SrCl (0.99 Å^{-1}) and $SrCl_2$ (0.87 Å^{-1}) molecules (vide supra).

Geometry and harmonic vibrational frequencies of $SrCl_2$ trapped in inert-gas matrices: the structure of $SrCl_2$·Ar$_n$ (n=1–7) complexes: Most of the available spectroscopic information on $SrCl_2$ comes from matrix isolation infrared spectroscopy (vide supra). Considering the strong Lewis acid character of $SrCl_2$, it is quite possible that the $SrCl_2$ molecules and the neighboring matrix atoms interact. In fact, there have been indications before of significant host–guest interactions of floppy molecules trapped in matrices owing to which molecular symmetry, geometrical parameters and vibrational frequencies may change considerably[33] or even "electronic ground-state reversal" may happen.[34] Therefore, we carried out a series of calculations in which we simulated the matrix effects by calculating the structures of complexes of $SrCl_2$ with argon atoms: $SrCl_2$·Ar$_n$ (n = 1–7). This approach has recently been applied successfully to lanthanide trihalides,[35–37] alkali halides,[38] and other alkaline-earth halides[39] even though in these cases fewer noble-gas atoms were considered.

The interactions involving the electron-deficient metal and the argon atoms are substantially attractive while the electron-rich chlorine and argon (repulsive) interactions are weak. Other important aspects to be taken into account are the attractive Ar···Ar interactions that, even though weaker than the $SrCl_2$–Ar interactions, may make a significant contribution to the resulting $SrCl_2$·Ar$_n$ geometries (the binding energy for an Ar$_2$ cluster is 0.14 kcal mol^{-1}).

There are many structures that can be constructed for these complexes and we investigated only the ones that seemed to be energetically favorable. The $SrCl_2$–Ar attraction energy is largest when the argon atoms are placed in the plane perpendicular to the $SrCl_2$ molecular plane (about 2 kcal mol^{-1}). The Sr–Ar distance is the shortest and the Ar–Cl distance the longest in these cases. These structures are labeled as group **A** and they are the energetically favored ones for up to five coordinating atoms. We looked at two more types of structures because they are similar in energy to the group **A** structures. In one of them, two argon atoms lie in the molecular plane and the others in the plane perpendicular to it (group **B**). In the third group (**C**), which we considered only for larger complexes (n = 4–7), four coordinating argon atoms form a square pyramid with the strontium atom, distal to the chlorine atoms, and the additional ones are placed on the side of the chlorine atoms, in a plane perpendicular to the $SrCl_2$ molecular plane. Finally, since placing of the seventh argon atom in this structure does not seem to be energetically favorable, we also calcu-

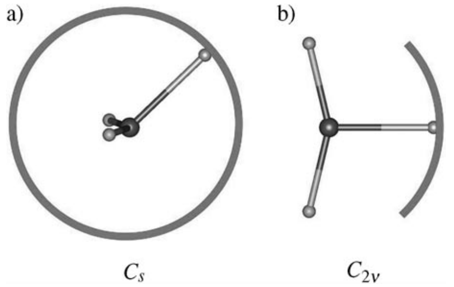

Figure 4. Areas in the $SrCl_2{\cdot}Ar$ complex energetically accessible to the argon atom. a) Along the circle in the plane bisecting the Cl-Sr-Cl bond angle. b) Along the arc in the molecular plane. The structure shown in (a) is the ground-state geometry for the $SrCl_2{\cdot}Ar$ complex (C_s); the structure in (b) is a transition state (C_{2v}).

lated the structure in which the seventh argon atom is attached to the strontium atom on the same side as the other four argon atoms, thus forming a square bipyramid on the side opposite to the chlorine atoms.

The $SrCl_2{\cdot}Ar$ complex: Preliminary single-point energy calculations of this molecule, by varying the angle between the Sr−Ar vector and the $SrCl_2$ plane (see Figure 4a), show very small energy variation (<1 kcal mol^{-1}) during a complete rotation, with two preferred orientations that are mirror images of each other through the molecular plane (one of them is shown in Figure 4a). Upon moving in the molecular plane, there are some regions in which it is advantageous for the argon atoms to link to the strontium atom to minimize the repulsive interactions with the chlorine atoms. This region is illustrated by the arc in Figure 4b. The C_{2v} structure, with the argon atom lying in the $SrCl_2$ plane, has an imaginary frequency that suggests distortion to the minimum energy structure shown in Figure 4a.

*Group **A** structures*: In this set of $SrCl_2{\cdot}Ar_n$ ($n=2$–6) structures the progressive coordination of argon atoms to strontium occurs exclusively in the plane that bisects the Cl-Sr-Cl bond angle (see Figure 5). Starting with the $SrCl_2{\cdot}Ar$ complex, the addition of successive argon atoms occurs adjacent to a linked one in order to maximize both Sr−Ar and Ar⋅⋅⋅Ar interactions. Thus an "Ar ring" is formed that surrounds the strontium atom when five or six inert-gas atoms are attached. For the complexes with up to four coordinating argon atoms the molecular shape of the $SrCl_2$ unit is only slightly perturbed while for the pentagonal bipyramid, $SrCl_2{\cdot}Ar_5$, and the hexagonal bipyramid, $SrCl_2{\cdot}Ar_6$, the $SrCl_2$ unit becomes linear to better accommodate all the argon atoms. Geometrical parameters and selected vibrational frequencies of the complexes are given in Table 3, while the Cartesian coordinates and further vibrational frequencies are given in the Supporting Information.

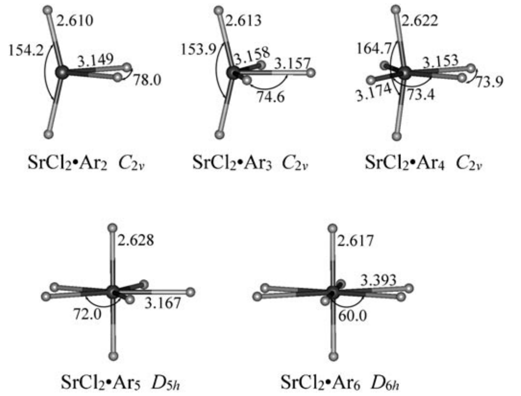

Figure 5. Molecular structures of $SrCl_2{\cdot}Ar_n$ ($n=2$–6) complexes (group **A**) and related geometrical parameters (distances in Å, angles in degrees).

Table 3. Molecular geometry, harmonic vibrational frequencies of the $SrCl_2$ fragment, and complexation energy of the $SrCl_2{\cdot}Ar_n$ ($n=1$–7) van der Waals complexes determined at the MP2//2f1g/2d2f1g/2d2f1g [Sr/Cl/Ar] level of theory.

	Symmetry	r(Sr−Cl) [Å]	∢Cl-Sr-Cl [°]	ΔE[a] [kcal mol^{-1}]	ν_1 [cm^{-1}]	ν_2 [cm^{-1}]	ν_3 [cm^{-1}]
$SrCl_2$	C_{2v}	2.603	153.5		277.0	32.4	324.5
Ar_2	$D_{\infty h}$	3.770	–	−0.14			
$SrCl_2{\cdot}Ar$	C_s	2.606	152.7	−2.2	275.3	33.6	322.4
Group **A**							
$SrCl_2{\cdot}Ar_2$	C_{2v}	2.610	154.2	−4.6	272.4	32.8	320.4
$SrCl_2{\cdot}Ar_3$	C_{2v}	2.613	153.9	−6.9	270.7	31.5	318.2
$SrCl_2{\cdot}Ar_4$	C_{2v}	2.622	164.7	−8.8	264.1	27.3	314.8
$SrCl_2{\cdot}Ar_5$	D_{5h}	2.628	180.0	−11.0			
$SrCl_2{\cdot}Ar_6$	D_{6h}	2.617	180.0	−10.8			
Group **B**							
$SrCl_2{\cdot}Ar_2$[b]	C_{2v}	2.601	140.0	−3.2	280.4	52.0	319.4
$SrCl_2{\cdot}Ar_3$[b]	C_s	2.604	139.7	−5.9	278.6	52.1	317.3
$SrCl_2{\cdot}Ar_4$	C_{2v}	2.607	139.7	−8.6	276.6	51.4	315.3
$SrCl_2{\cdot}Ar_5$	C_s	2.611	141.4	−10.3			
$SrCl_2{\cdot}Ar_6$	C_{2v}	2.622	151.9	−11.8	262.5	48.1 (58.4)	309.4
Group **C**							
$SrCl_2{\cdot}Ar_4$[b]	C_{2v}	2.602	132.5	−6.8	280.9	56.6	313.9
$SrCl_2{\cdot}Ar_5$	C_s	2.605	132.7	−9.3			
$SrCl_2{\cdot}Ar_6$	C_{2v}	2.609	133.8	−11.7			
$SrCl_2{\cdot}Ar_7$ **1**	C_{2v}	2.617	141.2	−12.6			
$SrCl_2{\cdot}Ar_7$ **2**	C_{2v}	2.609	133.3	−13.2			
Exp. Ar[c]			130 ± 5		275		308
Exp. Kr[d]			118 ± 5		269	44	300

[a] The stabilization energy corrected for BSSE has been computed with respect to the isolated $SrCl_2$ and argon atoms. [b] These structures have an imaginary frequency which suggests structural rearrangement toward the group **A** $SrCl_2{\cdot}Ar_2$ (C_{2v}) and $SrCl_2{\cdot}Ar_3$ (C_{2v}) and group **B** $SrCl_2{\cdot}Ar_4$ (C_{2v}) structures, respectively. [c] Ref. [16]. [d] Ref. [17].

High-symmetry structures, such as the square bipyramid, D_{4h}, for $SrCl_2{\bullet}Ar_4$, the trigonal bipyramid, D_{3h}, for $SrCl_2{\bullet}Ar_3$, and the square planar, D_{2h}, for $SrCl_2{\bullet}Ar_2$, are energetically disfavored for two reasons. On the one hand, the $SrCl_2$ molecule itself prefers a bent structure and therefore its alignment requires energy, and on the other, the distances between the argon atoms are too long in these structures to obtain a significant energy gain from the Ar⋅⋅⋅Ar interactions.

Comparison of the complex formation energies, corrected for BSSE, indicates a monotonic increase in exothermicity with an increasing number of argon atoms except for the last member of the group, the hexagonal bipyramid, $SrCl_2{\bullet}Ar_6$ (see Figure 6 and Table 3). For this structure the energy increases because the six argon atoms get too close to each other and the sixth Sr−Ar stabilizing interaction does not compensate for the repulsive Ar⋅⋅⋅Ar interactions. In fact, the Ar⋅⋅⋅Ar contacts in this complex (3.393 Å) are significantly shorter than the optimum value (3.770 Å) in the Ar_2 cluster. This results in a substantial elongation of the Sr−Ar distance in $SrCl_2{\bullet}Ar_6$ (3.393 Å) by more than 0.2 Å relative to the Sr−Ar distance in the other complexes (around 3.16 Å) with fewer argon atoms. Thus, in this $SrCl_2{\bullet}Ar_n$ series, the $SrCl_2{\bullet}Ar_5$ complex is the optimal one.

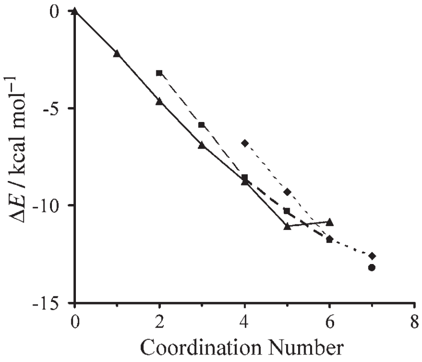

Figure 6. Calculated $SrCl_2{\cdots}Ar_n$ interaction energies for groups **A** [solid line; $SrCl_2{\bullet}Ar_n$ ($n=1$–6)], **B** [dashed line; $SrCl_2{\bullet}Ar_n$ ($n=2$–6)], and **C** [dotted line; for $SrCl_2{\bullet}Ar_n$ ($n=4$–7)] complexes (the second $SrCl_2{\bullet}Ar_7$ complex is indicated by a circle). The stabilization energies have been computed with respect to the isolated $SrCl_2$ molecule and the isolated number of argon atoms, n, with BSSE correction.

*Group **B** structures*: The second set of $SrCl_2{\bullet}Ar_n$ ($n=2$–6) complexes is characterized by two argon atoms in the $SrCl_2$ molecular plane with the remaining argon atoms lying in the plane bisecting the Cl-Sr-Cl bond angle (see Figure 7). For all these structures the $SrCl_2$ unit remains bent; the Cl-Sr-Cl bond angle first decreases relative to that in the isolated $SrCl_2$ molecule because of the "pressure" of the two argon atoms placed in the molecular plane; then, for the complexes with five and six argon atoms, the angle increases again because the additional argon atoms are placed between the two chlorine atoms. The Sr−Ar distances in the $SrCl_2$ plane are larger (about 3.3–3.4 Å) than the other ones (about 3.15–3.22 Å) and this leads to the lower stability of the **B** $SrCl_2{\bullet}Ar_n$ (n up to 5) complexes compared with the corresponding **A** ones (Figure 6 and Table 3). In fact, two of the **B** structures, $SrCl_2{\bullet}Ar_2$ and $SrCl_2{\bullet}Ar_3$, are not stable minima but transition-state structures with one imaginary frequency and this suggests their structural rearrangement towards the **A** structures. At the same time, the **B** $SrCl_2{\bullet}Ar_6$ arrangement is more stable than the corresponding **A** structure. This complex has the largest number of relatively short Sr−Ar contacts (two of 3.158 Å and two others of 3.253 Å, compared with the six Sr−Ar distances of 3.393 Å in the **A** $SrCl_2{\bullet}Ar_6$ complex). In this molecule the strontium atom reaches its optimum coordination number of eight.[40] With eight-coordination, the primary coordination sphere may be saturated and additional argon atoms will bind in the second coordination sphere with decreasing strength of attachment.

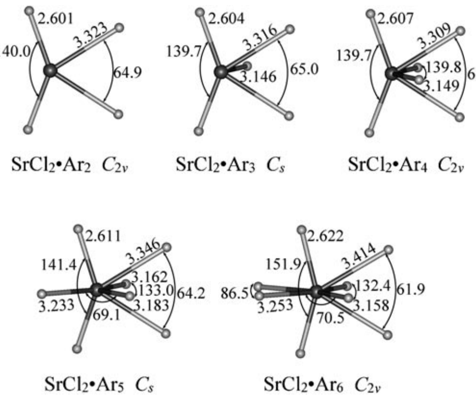

Figure 7. Molecular structures of $SrCl_2{\bullet}Ar_n$ ($n=2$–6) complexes (group **B**) and related geometrical parameters (distances in Å, angles in degrees).

*Group **C** structures*: In these structures four argon atoms form a square pyramid with the strontium atom on the side opposite the chlorine atoms, while the coordination of further argon atoms happens between the chlorine atoms in the plane bisecting the Cl-Sr-Cl bond angle (Figure 8).

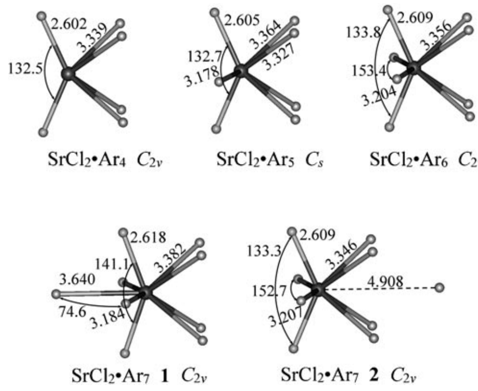

Figure 8. Molecular structures of the $SrCl_2{\bullet}Ar_n$ ($n=4$–7) complexes (group **C**) and related geometrical parameters (distances in Å, angles in degrees).

These structures are somewhat similar to the **B** structures in that the $SrCl_2$ molecule is bent and the Cl-Sr-Cl bond angle is smaller than the one in the free molecule. The bond angle is also smaller than the one in the homologous **B** complexes, thus indicating that the four argon atoms distal to the chlorine atoms exercise a higher "pressure" on the $SrCl_2$ molecule (Figure 8 and Table 3). The Sr−Ar distances of the Sr−Ar square-pyramid moiety in the complexes containing four and five argon atoms are somewhat (about 0.03 Å) longer than the Sr−Ar distances in the molecular plane of the corresponding **B** structures. They are considerably longer (by almost 0.2 Å) than the Sr−Ar distances in the plane perpendicular to the molecule in the **B** structures. Accordingly, the $SrCl_2{\cdot}Ar_4$ complex is considerably (about 2–3 $kcal\,mol^{-1}$) less stable than the homologous **A** and **B** complexes (Figure 6 and Table 3) and our vibrational analysis gives an imaginary frequency indicating distortion towards the $SrCl_2{\cdot}Ar_4$ **B** complex. For the larger complexes the energy difference between the **C** complexes and the homologous **A** and **B** structures decreases and for $SrCl_2{\cdot}Ar_6$ the energies of the **B** and **C** structures are about the same (Figure 6 and Table 3). For group **C** we also calculated the structure of the $SrCl_2{\cdot}Ar_7$ complex with nine-coordination around the strontium atom. Although in this molecule the new Sr−Ar distance is rather long (3.64 Å), the coordination of the additional argon atom introduces a further energy gain and opens the Cl-Sr-Cl bond angle by about 7° with respect to the $SrCl_2{\cdot}Ar_6$ **C** complex.

Finally, we also calculated the structure in which the seventh argon atom attaches to the base of the $SrAr_4$ square pyramid (**2**, see Figure 8). The geometrical parameters of the $SrCl_2$ part of this complex are similar to the group **C** $SrCl_2{\cdot}Ar_6$ complex while the Sr−Ar bonds of the square pyramid are about 0.04 Å shorter than those in structure **1**. The seventh argon atom here clearly belongs to the second coordination sphere with a Sr···Ar distance of 4.908 Å. Interestingly, the formation energy of this complex after BSSE correction is more exothermic than that of the corresponding **C** complex, **1** (see Figure 6). This can be explained easily by the strain introduced into the complex by the seventh argon atom being in the plane of the two other argon atoms on the side of the two chlorine atoms in **1**. Thus, apparently, structure **2** takes us closest to the possible structure of the complex that might be formed between the $SrCl_2$ molecule and the host argon atoms in the matrix.

Discussion

Gas-phase structure of $SrCl_2$: The alkaline-earth dihalide molecules closest to $SrCl_2$ as far as their shapes are concerned, namely, CaF_2 and $SrBr_2$, are extremely floppy, have a very small bending frequency and are characterized as typical quasilinear molecules.[13,8] $SrCl_2$ occupies an interesting position in between these two molecules. $SrBr_2$ was found to be linear by electron diffraction analysis but with a very shallow bending potential: even bending the molecule by 10° required less than 0.2 $kcal\,mol^{-1}$ energy.[8] CaF_2 was found to be bent with a barrier to linearity of 54 cm^{-1}, which strongly depends on electron correlation effects.[13] We calculated the barrier to linearity for $SrCl_2$ by different methods and the results are shown in Figure 9. Apparently, the molecule is linear at the HF level of theory, but becomes bent at the correlated levels, as both the MP2 and DFT calculations indicate, in agreement with what was found for CaF_2. The barrier to linearity is about three times larger by the B3PW91 calculation than by the MP2 one. The MP2 barrier is about 35 cm^{-1}, that is, barely 10 cm^{-1} (0.03 kcal mol^{-1}) larger than the computed bending frequency of $SrCl_2$. Considering the usual insensitivity of different computational methods to very small frequencies, $SrCl_2$ appears to be a quasilinear molecule.

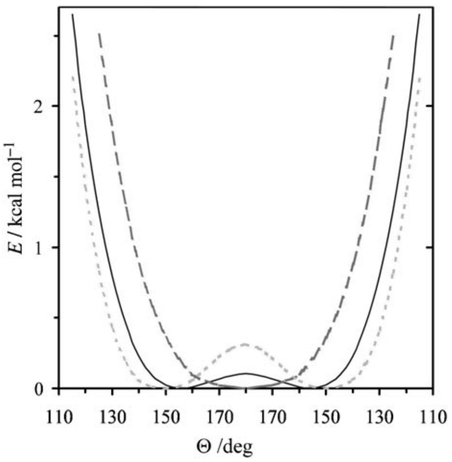

Figure 9. The bending potential of $SrCl_2$ at different levels of theory (dashed line: HF; solid line: MP2; dotted line: B3PW91). Applied basis sets are: Sr: 4f3g1h; Cl: cc-pV5Z.

The computed geometrical parameters of a molecule such as $SrCl_2$ depend strongly on the method and basis sets applied. The usual practice for such systems is to increase the level of computation until a convergence is reached in the geometrical parameters; this is called the complete basis set (CBS) limit. We could not reach such a convergence for $SrCl_2$, at least not with the correlated methods. Interestingly, the density functional calculations seem to converge at 2.606 Å and 148.9°. However, neither the MP2 nor the few CCSD(T) calculations do so. For the MP2 calculations even the last change in the basis set from 4f3g2h/cc-pV5Z to 4f3g2h1i/cc-pV(6+d)Z brings about a 0.004 Å decrease in the Sr−Cl bond length (Table 1), which, in fact, is larger than the previous step of 0.002 Å. Thus, we still cannot talk about convergence here. With the CCSD(T) calculations we could not afford these very large basis sets, but we can estimate the possible effect of their increase from a comparison of the basis set expansion effect for the MP2 and CCSD(T) calculations at the lower levels of theory. From this comparison we might estimate a bond length of 2.604 Å for the

CCSD(T) calculation with the largest basis set applied here. The bond angle does not seem to converge at all, so we cannot even estimate its convergence.

We would like to give a bond length and bond angle that could be considered as best describing the computed equilibrium geometry of this molecule. Because of the apparent difficulties in the convergence discussed above, we used a somewhat arbitrary approach and calculated the weighted mean of our results with its appropriate standard deviation. For the weighting system we considered the total energies after subtracting the contribution of atomic energies (for details of this calculation see the Supporting Information). Only the bent structures were taken into account. Our final calculated equilibrium bond length is 2.605 ± 0.006 Å and the bond angle is $153.5 \pm 2.6°$.

The experimental electron diffraction geometry is a thermal average structure, while the computed one is the equilibrium structure that describes a motionless molecule at 0 K. The higher the experimental temperature and the more extensive the floppiness of the molecule, the larger the difference between the thermal average and the equilibrium geometries is.[18] For $SrCl_2$ both are important factors. In order to compare the two structures we approached the question from both sides. From the electron diffraction side we estimated the experimental equilibrium structure by applying anharmonic corrections in two different ways (vide supra). The estimated equilibrium distance determined by electron diffraction is 2.607 ± 0.013 and 2.606 ± 0.008 Å from the two methods and these agree well with the computed Sr−Cl bond length (2.605 ± 0.006 Å).

We also tried to estimate the thermal average bond length from the computation which is a more difficult task because of the applied one-dimensional approach. According to the potential energy curve of the symmetric stretching mode (Figure 3a), the bond length increases by about 0.012 Å giving a thermal average bond length of 2.613 Å at the MP2/4f3g1h/cc-pV5Z level for the temperature of the ED experiment, 1500 K. The asymmetric stretching does not seem to contribute to the change in bond length, at least not at the primary level. At the same time, the strong but negative anharmonic bending brings about a bond shortening with increasing temperature, eventually amounting to 0.008 Å (0.005 Å at the B3PW91 level) at 1500 K. It is not clear what the overall outcome of these two opposite effects would be since the coupling of the vibrations has not been considered in our treatment. Nonetheless, the strong anharmonic character of the symmetric stretching suggests that we can expect a certain amount of bond lengthening at 1500 K, the temperature of the experiment, in agreement with our findings, even if the actual lengthening does not quite reach the measured thermal average bond length of 2.625 ± 0.010 Å.

The experimental thermal average bond angle is about 10° smaller ($142.4 \pm 4.0°$) than the computed equilibrium bond angle ($153.5 \pm 2.6°$). Analysis of the bending potential results in a strong reduction of the bond angle to 146.5 (MP2) and 144.9° (B3PW91) upon increasing the temperature, showing excellent agreement between the two methods. The large uncertainty in the ED bond angle comes from the fact that the Cl···Cl contribution to the molecular scattering is too small (vide supra).

Concerning the comparison of structural parameters derived from experiment and computation, the estimated equilibrium bond length from electron diffraction is in good agreement with the computed results. Because of the large experimental error in the bond angle, a similar comparison was not attempted for it. The opposite is true for the computation. The estimation of the thermal average bond angle by the analysis of the anharmonic bending motion of the molecule gives good agreement with experiment. At the same time, the estimation of the thermal average bond length, due to opposite influences of the stretching and bending modes on it, hindered a similar comparison as the necessary information on the coupling of the different vibrational modes was lacking.

Matrix effect on the structure of $SrCl_2$: Vibrational spectroscopic experiments carried out in different inert-gas matrices may have measured a structure that is different from that of the isolated gas-phase molecule due to possible interactions with the matrix atoms.[16,17] The strong Lewis acid character of $SrCl_2$ and the large polarizability of the strontium atom also support the possibility of host–guest interactions in these matrices. In order to check this possibility, we have simulated the matrix environment by computing the structures and for some of them the vibrational frequencies of the $SrCl_2{\cdot}Ar_n$ ($n = 1$–7) complexes.

For all three sets of $SrCl_2{\cdot}Ar_n$ structures the complex formation energies (Table 3) indicate that the argon atoms are strongly coordinated to the metal and that their presence induces important geometrical changes in the structure of the $SrCl_2$ molecule. The Mulliken charges calculated for the $SrCl_2{\cdot}Ar_n$ complexes (see Figure S1–S4 in the Supporting Information) suggest ion-induced dipole interactions with substantial electron-density transfer from the argon atoms to the $SrCl_2$ molecule.

For the **A** structures the coordination of argon atoms leads to a noticeable increase in the Sr−Cl bond lengths. This can be rationalized in terms of the $Ar_n \rightarrow SrCl_2$ electron-density transfer, which slightly destabilizes the $SrCl_2$ molecular orbitals and weakens the Sr−Cl bonds, and by the opening of the Cl−Sr−Cl angle which favors bond lengthening. The Sr−Cl bond length gradually increases with an increasing number of coordinating argon atoms except for $SrCl_2{\cdot}Ar_6$, for which the weaker and longer Sr···Ar interactions do not make this necessary. These geometry changes are accompanied by a small and gradual decrease of both stretching modes. In the **A** structures the $SrCl_2$ part of the molecule remains flexible along the bending motion (up to the $SrCl_2{\cdot}Ar_4$ complex) and the potential energy curve is very flat. The bond angle changes considerably with an increase in the number of coordinating argon atoms. The ν_2 bending frequency for the $SrCl_2{\cdot}Ar_2$ and $SrCl_2{\cdot}Ar_3$ complexes is similar to that of the isolated $SrCl_2$ molecule, but it decreases for the larger complexes as the bond angle opens (see $SrCl_2 \cdot Ar_4$).

The geometry changes in the $SrCl_2$ unit are quite different for the **B** structures. The Sr–Cl bond length does not change in the first two complexes as a result of two competing effects: the $Ar_n \rightarrow SrCl_2$ electron-density transfer would cause bond elongation just as in the **A** structures, but the decrease in the bond angle, caused by the new Sr···Ar interactions in the molecular plane, compensates for that. For the larger complexes in this group, the Sr–Cl bond lengthens but to a smaller extent than in the **A** structures (except for the $SrCl_2 \cdot Ar_6$ complex). The symmetric stretching frequency does not change much in keeping with the small change in the bond length.

For the structures of the **B** and especially the **C** groups the bond angles are smaller than in the gaseous $SrCl_2$ molecule. As a consequence, the ν_2 harmonic frequencies are considerably larger than that in the free molecule. In the **B** structures the two argon atoms in the molecular plane considerably affect the bending motion and make the $SrCl_2$ molecule stiffer, while in the **C** structures the four connecting argon atoms opposite the chlorine atoms have the same effect. The frequency shifts computed for the **C** complex, $SrCl_2 \cdot Ar_4$, are similar to those of the **B** $SrCl_2 \cdot Ar_4$ complex because the structural changes in the $SrCl_2$ unit are also similar. The substantial, about 20°, decrease in the bond angle with respect to the isolated $SrCl_2$ molecule results in a considerably (about $20\,cm^{-1}$) larger bending frequency in the complex. At the same time, the symmetric stretching frequency increases only slightly, while the asymmetric stretching decreases by almost $10\,cm^{-1}$.

In summary, owing to the exothermic nature of the $SrCl_2$ and argon interactions, they, indeed, may take place during matrix isolation experiments. Moreover, according to the relative energies of the different $SrCl_2 \cdot Ar_n$ molecules, complexes with more argon atoms, at least five, six or even seven, are expected to form. The species with six argon atoms accomplish the eight coordination of strontium which appears to be the favorite coordination number of this element in its crystal form. Crystals of strontium compounds with a coordination number of nine exist, corresponding to complexes with seven argon atoms. The overall lowest energy is achieved for the complex having seven argon atoms in a square-bipyramidal arrangement (see Figure 8). Since the $SrCl_2$ part of this molecule has about the same structure as the **C** $SrCl_2 \cdot Ar_4$ complex, we may expect vibrational frequencies similar to its $SrCl_2$ part (see Table 3, we could not calculate the frequencies of the complex with seven argon atoms). This eliminates the large discrepancy between the experimental and the computed asymmetric stretching frequencies of $SrCl_2$ (measured in argon matrix: $308\,cm^{-1}$; free $SrCl_2$ molecule, computed: $322\,cm^{-1}$; $SrCl_2 \cdot Ar_4$: $313\,cm^{-1}$) and shows that complex formation in the matrix may seriously influence the measured frequencies. Apparently, from our models, the **C** complexes with more (at least four) coordinating argon atoms simulate the matrix effects better than the group **A** structures.

Finally, it is worth mentioning that experimental vibrational frequencies have also been measured for $SrCl_2$ in a krypton matrix.[17] As the polarizability of krypton is greater than that of argon, we may expect a larger change in the frequencies relative to the gas-phase values and, in fact, this is what we observe.

Acknowledgements

Judit Molnár and Annamarie McKenzie participated in the initial stages of this study and we appreciate their contribution. M.H. and Z.V. thank the Hungarian Scientific Research Fund (OTKA T037978 and OTKA 060365) for support and the National Information Infrastructure Development Program of Hungary for additional computer time.

---

[1] Although there have been attempts to explain the anomalous behavior of alkaline-earth dihalides with the VSEPR model using the distortion of the electron density of the (n–1) core: R. J. Gillespie, I. Hargittai, *The VSEPR Model of Molecular Geometry*, Allyn and Bacon, Boston, **1992**.

[2] A. D. Walsh, *J. Chem. Soc.* **1953**, 2266–2288.
[3] E. P. F. Lee, T. G. Wright, *J. Phys. Chem. A* **2000**, *104*, 974–981.
[4] a) N. Vogt, G. V. Girichev, J. Vogt, A. G. Girichev, *J. Mol. Struct.* **1995**, *352/353*, 175–179; b) A. G. Girichev, N. I. Giricheva, N. Vogt, *J. Mol. Struct.* **1996**, *384*, 175–182; c) N. I. Giricheva, G. V. Girichev, A. G. Girichev, *Struct. Chem.* **2000**, *11*, 313–318.
[5] a) J. Molnár, C. J. Marsden, M. Hargittai, *J. Phys. Chem.* **1995**, *99*, 9062–9071; b) B. Réffy, M. Kolonits, M. Hargittai, *J. Phys. Chem. A* **2005**, *109*, 8379–8384.
[6] E. Vajda, M. Hargittai, I. Hargittai, J. Tremmel, J. Brunvoll, *Inorg. Chem.* **1987**, *26*, 1171–1174.
[7] M. Hargittai, M. Kolonits, G. Schultz, *J. Mol. Struct.* **2001**, *567/568*, 241–246.
[8] M. Hargittai, M. Kolonits, D. Knausz, I. Hargittai, *J. Chem. Phys.* **1992**, *96*, 8980–8985.
[9] M. Hargittai, *Chem. Rev.* **2000**, *100*, 2233–2301.
[10] M. Kaupp, P. v. R. Schleyer, H. Stoll, H. Preuss, *J. Am. Chem. Soc.* **1991**, *113*, 6012–6020.
[11] L. Seijo, Z. Barandiaran, S. Huzinaga, *J. Chem. Phys.* **1991**, *94*, 3762–3773.
[12] M. Hargittai, *Coord. Chem. Rev.* **1988**, *91*, 35–88.
[13] J. Koput, A. Roszczak, *J. Phys. Chem. A* **2004**, *108*, 9267–9273.
[14] V. P. Spiridonov, A. B. Altman, A. G. Gershikov, G. V. Romanov, *2nd Conference on the Determination of Molecular Structure by Microwave Spectroscopy and Electron Diffraction*, Tübingen (Germany), **1980**.
[15] V. I. Baikov, *Opt. Spektrosk.* **1969**, *27*, 923–929.
[16] J. W. Hastie, R. H. Hauge, J. L. Margrave, *High Temp. Sci.* **1971**, *3*, 56–72.
[17] D. White, G. V. Calder, S. Hemple, D. E. Mann, *J. Chem. Phys.* **1973**, *59*, 6645–6651.
[18] M. Hargittai, I. Hargittai, *Int. J. Quantum Chem.* **1992**, *44*, 1057–1067.
[19] Gaussian 03 (Revision B.05), M. J. Frisch, G. W. Trucks, H. B. Schlegel, G. E. Scuseria, M. A. Robb, J. R. Cheeseman, J. A. Montgomery, Jr., T. Vreven, K. N. Kudin, J. C. Burant, J. M. Millam, S. S. Iyengar, J. Tomasi, V. Barone, B. Mennucci, M. Cossi, G. Scalmani, N. Rega, G. A. Petersson, H. Nakatsuji, M. Hada, M. Ehara, K. Toyota, R. Fukuda, J. Hasegawa, M. Ishida, T. Nakajima, Y. Honda, O. Kitao, H. Nakai, M. Klene, X. Li, J. E. Knox, H. P. Hratchian, J. B. Cross, C. Adamo, J. Jaramillo, R. Gomperts, R. E. Stratmann, O. Yazyev, A. J. Austin, R. Cammi, C. Pomelli, J. W. Ochterski, P. Y. Ayala, K. Morokuma, G. A. Voth, P. Salvador, J. J. Dannenberg, V. G. Zakrzewski, S. Dapprich, A. D. Daniels, M. C. Strain, O. Farkas, D. K. Malick, A. D. Rabuck, K. Raghavachari, J. B. Fores-

man, J. V. Ortiz, Q. Cui, A. G. Baboul, S. Clifford, J. Cioslowski, B. B. Stefanov, G. Liu, A. Liashenko, P. Piskorz, I. Komaromi, R. L. Martin, D. J. Fox, T. Keith, M. A. Al-Laham, C. Y. Peng, A. Nanayakkara, M. Challacombe, P. M. W. Gill, B. Johnson, W. Chen, M. W. Wong, C. Gonzalez, J. A. Pople, Gaussian, Inc., Pittsburgh, PA, **2003**.

[20] P. J. Hay, W. R. Wadt, *J. Chem. Phys.* **1985**, *82*, 299–310.

[21] M. Kaupp, P. v. R. Schleyer, H. Stoll, H. Preuss, *J. Chem. Phys.* **1991**, *94*, 1360–1366.

[22] A. D. McLean, G. S. Chandler, *J. Chem. Phys.* **1980**, *72*, 5639–5648.

[23] B. Reffy, C. J. Marsden, M. Hargittai, *J. Phys. Chem. A* **2003**, *107*, 1840–1849.

[24] D. E. Woon, T. H. Dunning, Jr., *J. Chem. Phys.* **1993**, *98*, 1358–1371.

[25] T. H. Dunning, Jr., K. A. Peterson, A. K. Wilson, *J. Chem. Phys.* **2001**, *114*, 9244–9253.

[26] V. Barone, A. Grand, C. Minichino, R. Subra, *J. Chem. Phys.* **1993**, *99*, 6787–6798.

[27] a) I. Hargittai, J. Tremmel, M. Kolonits, *HSI Hung. Sci. Instrum.* **1980**, *50*, 31–42; b) I. Hargittai, S. Bohatka, J. Tremmel, I. Berecz, *HSI Hung. Sci. Instrum.* **1980**, *50*, 51–56.

[28] J. Tremmel, I. Hargittai, *J. Phys. E* **1985**, *18*, 148–150.

[29] A. W. Ross, M. Fink, R. Hilderbrandt, J. Wang, V. H. Smith, Jr. in *International Tables for Crystallography, Vol. C* (Ed.: A. J. C. Wilson), Kluwer, Dordrecht, **1995**, pp. 245–338.

[30] L. S. Bartell, *J. Chem. Phys.* **1955**, *23*, 1219–1222.

[31] A. G. Gershikov, *Khim. Fiz.* **1982**, *1*, 587–593.

[32] K. Kuchitsu, Y. Morino, *Bull. Chem. Soc. Jpn.* **1965**, *38*, 805–813.

[33] I. R. Beattie, P. J. Jones, N. A. Young, *Mol. Phys.* **1991**, *72*, 1309–1312.

[34] L. Andrews, B. Y. Liang, J. Li, B. E. Bursten, *J. Am. Chem. Soc.* **2003**, *125*, 3126–3139.

[35] G. Lanza, C. Minichino, *J. Phys. Chem. A* **2004**, *108*, 4949–4960.

[36] G. Lanza, C. Minichino, *ChemPhysChem* **2004**, *5*, 120–123.

[37] G. Lanza, C. Minichino, *J. Phys. Chem. A* **2005**, *109*, 2127–2138.

[38] R. L. Redington, *J. Chem. Phys.* **1995**, *102*, 7332–7340.

[39] M. Kaupp, P. v. R. Schleyer, H. Stoll, *J. Phys. Chem.* **1992**, *96*, 9801–9805.

[40] $SrCl_2$ has the fluorite-type crystal structure in which the metal is coordinated to eight halogen atoms and strontium prefers a coordination number of eight in its complexes as well: A. F. Wells, *Structural Inorganic Chemistry*, 4th ed., Clarendon Press, Oxford, **1975**.

Received: March 8, 2006